

RESEARCH ARTICLE

Essentiality of *Plasmodium falciparum* plasmepsin V

Nonlawat Boonyalai^{1†*}, Christine R. Collins², Fiona Hackett², Christlaine Withers-Martinez², Michael J. Blackman^{2,3*}

1 Department of Biochemistry, Faculty of Science, Kasetsart University, Chatuchak, Bangkok, Thailand, **2** Malaria Biochemistry Laboratory, The Francis Crick Institute, London, United Kingdom, **3** Department of Pathogen Molecular Biology, London School of Hygiene & Tropical Medicine, London, United Kingdom

† Current address: Department of Immunology and Medicine, US Army Medical Directorate-Armed Forces Research Institute of Medical Science (USAMD-AFRIMS), Bangkok, Thailand.

* nonlawat.b@ku.ac.th(NB), nonlawatb.ca@afirms.org; mike.blackman@crick.ac.uk(MJB)



OPEN ACCESS

Citation: Boonyalai N, Collins CR, Hackett F, Withers-Martinez C, Blackman MJ (2018) Essentiality of *Plasmodium falciparum* plasmepsin V. PLoS ONE 13(12): e0207621. <https://doi.org/10.1371/journal.pone.0207621>

Editor: Gordon Langsley, Institut national de la santé et de la recherche médicale - Institut Cochin, FRANCE

Received: June 14, 2018

Accepted: November 2, 2018

Published: December 5, 2018

Copyright: © 2018 Boonyalai et al. This is an open access article distributed under the terms of the [Creative Commons Attribution License](https://creativecommons.org/licenses/by/4.0/), which permits unrestricted use, distribution, and reproduction in any medium, provided the original author and source are credited.

Data Availability Statement: All relevant data are within the paper and its Supporting Information files.

Funding: This work was supported by a Royal Society Newton Mobility Grant (NI160028; <https://royalsociety.org/>) and by the Office of Higher Education Commission, Thailand (to NB). The work was also supported by the Francis Crick Institute (to MJB; <https://www.crick.ac.uk/>) which receives its core funding from Cancer Research UK (FC001043; <https://www.cancerresearchuk.org/>).

Abstract

The malaria parasite replicates within erythrocytes. The pathogenesis of clinical malaria is in large part due to the capacity of the parasite to remodel its host cell. To do this, intraerythrocytic stages of *Plasmodium falciparum* export more than 300 proteins that dramatically alter the morphology of the infected erythrocyte as well as its mechanical and adhesive properties. *P. falciparum* plasmepsin V (PfPMV) is an aspartic protease that processes proteins for export into the host erythrocyte and is thought to play a key role in parasite virulence and survival. However, although standard techniques for gene disruption as well as conditional protein knockdown have been previously attempted with the *pfpmv* gene, complete gene removal or knockdown was not achieved so direct genetic proof that PMV is an essential protein has not been established. Here we have used a conditional gene excision approach combining CRISPR-Cas9 gene editing and DiCre-mediated recombination to functionally inactivate the *pfpmv* gene. The resulting mutant parasites displayed a severe growth defect. Detailed phenotypic analysis showed that development of the mutant parasites was arrested early in the ring-to-trophozoite transition in the erythrocytic cycle following gene excision. Our findings are the first to elucidate the effects of PMV gene disruption, showing that it is essential for parasite viability in asexual blood stages. The mutant parasites can now be used as a platform to further dissect the *Plasmodium* protein export pathway.

Introduction

Malaria was responsible for approximately 445,000 deaths and 216 million clinical cases in 2016, an increase of ~5 million cases over the previous year [1]. Vital to the growth and pathogenicity of the parasite is host cell remodelling in which the parasite modifies the host erythrocyte by the synthesis and export of over 300 parasite proteins beyond the bounds of the parasitophorous vacuole (PV) within which it replicates (for reviews see [2, 3]). The exported proteins are trafficked from the parasite to the host erythrocyte via a putative parasite-derived

the UK Medical Research Council (FC001043; <https://www.mrc.ac.uk/>), and the Wellcome Trust (FC001043; <https://wellcome.ac.uk/>). The authors also acknowledge Wellcome ISSF2 funding to the London School of Hygiene & Tropical Medicine. The funders had no role in study design, data collection and analysis, decision to publish, or preparation of the manuscript.

Competing interests: The authors have declared that no competing interests exist.

protein complex known as the translocon of exported proteins (PTEX), located within the PV membrane (PVM) [4–9]. The exported proteins extensively alter the mechanical and adhesive properties of infected erythrocytes, resulting in vascular sequestration of the infected cells and eventual destruction of the host erythrocyte [10]. Protein export in *Plasmodium* has been most intensively studied in *P. falciparum* (reviewed in [11, 12]), where the majority of known exported proteins contain the pentameric localisation motif RxLxE/Q/D, termed *Plasmodium* export element (PEXEL), typically located downstream of the N-terminal secretory signal sequence that regulates entry into the ER [13, 14]. Some proteins lacking a PEXEL motif, referred to as PEXEL-negative exported proteins (PNEPs), can also be exported through a distinct mechanism that may however share features with PEXEL-mediated export [15, 16].

P. falciparum plasmepsin V (PfPMV) is an ER-located aspartic protease comprising 590 amino acid residues (~68 kDa) [17]. PfPMV expression levels in the parasite progressively increase throughout schizogony [17]. Numerous studies have now established that PMV is directly responsible for cleavage of the PEXEL motif within exported proteins [18–21]. Cleavage occurs on the C-terminal side of the conserved Leu residue (RxL↓), revealing a new N-terminus that is rapidly acetylated (^{Ac}-xE/Q/D) [22, 23]. A recent x-ray crystal structure of *Plasmodium vivax* PMV (PvPMV) revealed a canonical aspartyl protease fold with several important features [24]. These include a nepenthesin (NAP)-like insertion within the N-terminal part of the enzyme, which may control substrate entry into the active site and influence enzyme specificity, as well as a helix-turn-helix (HTH) motif near the C-terminus of the enzyme, which is conserved in PMV from other *Plasmodium* species but not found in other parasite plasmepsins involved in hemoglobin digestion. PMV also possesses an unpaired Cys residue (C140 in PvPMV, equivalent to C178 in the *P. falciparum* enzyme) which is located in the flap of the structure and is restricted to *Plasmodium* species. In attempts to establish the druggability and function of PMV, several peptidomimetic inhibitors based on the PEXEL motif have been developed [25–27]. A co-crystal structure of PMV bound to one of these compounds, the PEXEL-mimetic WEHI-842, showed that although the unpaired Cys points into the active site of the enzyme, it does not appear to make contact with the inhibitor [24, 28]. Another inhibitor, WEHI-916, inhibits the activity of purified PMV isolated from both *P. falciparum* and *P. vivax*, and higher concentrations of WEHI-916 were required to kill parasites engineered to over-express PfPMV indicating on-target efficacy [25, 27]. Compound 1, a hydroxyl-ethylamine PEXEL-mimetic, inhibited PfPMV activity in vitro with picomolar potency but failed to block parasite growth due to poor stability and membrane permeability [26]. Collectively, these findings indicate that PMV has a number of distinguishing features that could be exploited in drug design, and that it can potentially be targeted with suitable inhibitory compounds.

An important component in the validation of any enzyme as a drug target is genetic ablation of enzyme expression. Unfortunately, previous attempts to genetically delete or knock-down PMV expression have been only partially successful. Work by Klemba and colleagues [17] and Boddey et al [18] failed to disrupt the *pfpmv* gene or the *P. berghei* PMV gene (*pbpmv*) respectively, suggesting (but not proving) that the gene is essential. Russo et al [21] similarly attempted to disrupt the *pfpmv* gene using an allelic replacement approach. Single crossover homologous recombination into the endogenous *pfpmv* locus was possible only when the catalytic dyad aspartate codons were preserved. Conditional knockdown of PfPMV expression was also attempted using the RNA-degrading *glmS* ribozyme system [27]. Although this resulted in around 75–90% knockdown of PMV expression, the remaining PMV levels were presumably sufficient to enable export and sustain parasite development. Gambini et al [26] generated an inducible PMV knock-down by fusing PMV with a destabilising domain (DD), but only a 4 to 10-fold knock-down of PMV cellular levels was achieved using this

approach, which did not affect parasite viability. In summary, whilst some of these data are consistent with an essential role for PMV, in the absence of any reports of complete ablation of PfPMV expression, direct genetic proof that PMV is an essential protein is lacking.

Here we have used a robust conditional genetic approach to truncate the *pfpmv* gene. Our findings are the first to confirm genetically that disruption of PfPMV has a significant effect on ring-to-trophozoite development and ultimately results in arrest of parasite growth.

Results

Generation of modified *pfpmv* parasites using CRISPR-Cas9

Previous attempts to disrupt the *pfpmv* gene using conventional genetic techniques were unsuccessful [18, 21], and conditional knockdown approaches did not significantly affect PEXEL processing or parasite viability [26, 27], presumably due to relatively low levels of PfPMV expression being sufficient to sustain parasite viability. To explore the consequences of complete functional inactivation of PMV, we therefore took advantage of the DiCre conditional recombinase system, recently adapted to *P. falciparum* [29]. Using Cas9-mediated genome editing [30] we first introduced synthetic introns containing *loxP* sites (*loxPint* sequences; [31]) into the endogenous *pfpmv* locus such that they flanked (floxed) an internal segment of the gene encoding Asp133 to Thr590. Importantly, one of the PfPMV catalytic dyad residues (Asp365) is included within this floxed region. At the same time, the modified gene was fused to a C-terminal HA3 epitope tag to aid detection of the transgene product (Fig 1A). The repair plasmid used for the manipulation contains a modified selection-linked integration (SLI) region [32] which allows selection for integration events with neomycin. This is enabled by the integration of a 2A peptide sequence immediately downstream of the modified gene, which causes ribosome ‘skipping’ to produce two distinct polypeptides (the modified PMV-HA and the *neo-R* gene product) from a single mRNA (note that neomycin selection was in fact unnecessary in our work due to the high efficiency of the Cas9-mediated homologous recombination). The genomic modification was made in the DiCre-expressing *P. falciparum* B11 parasite clone [33] such that excision of the floxed sequence could be induced by treatment of the transgenic parasites with rapamycin (RAP). DiCre-mediated excision was predicted to generate an internally-truncated mutant form of PMV lacking one of the catalytic dyad residues. Excision would also remove the *neo-R* gene and induce expression of GFP as a fluorescent reporter of excision by virtue of a second downstream 2A peptide sequence (Fig 1A).

Successful modification of the *pfpmv* gene in the transfected parasite population following the introduction of the targeting vector was confirmed by diagnostic PCR. Limiting dilution cloning of the modified parasites resulted in the isolation of parasite clones PMV-C5 and PMV-F9, which were derived from independent transfections using different guide RNAs. Modification of the native *pfpmv* locus was confirmed in both transgenic parasite lines by diagnostic PCR (Fig 1B). Both clones replicated at a rate indistinguishable from that of the parental B11 parasites, suggesting that the modifications did not affect parasite viability. Transgenic parasite clone PMV-C5 was used for all subsequent experiments.

Conditional truncation of the *pfpmv* gene

Expression of the recodonised *pfpmv* gene in transgenic parasite clone PMV-C5 was expected to produce an epitope-tagged PMV product (called PMV-HA), as well as expression of the *neo-R* gene product. Note that in this event GFP is not produced because of the presence of a translational stop codon directly downstream of the *neo-R* gene. Upon RAP-treatment, site-specific recombination between the introduced *loxP* sites in the modified *pfpmv* locus of the

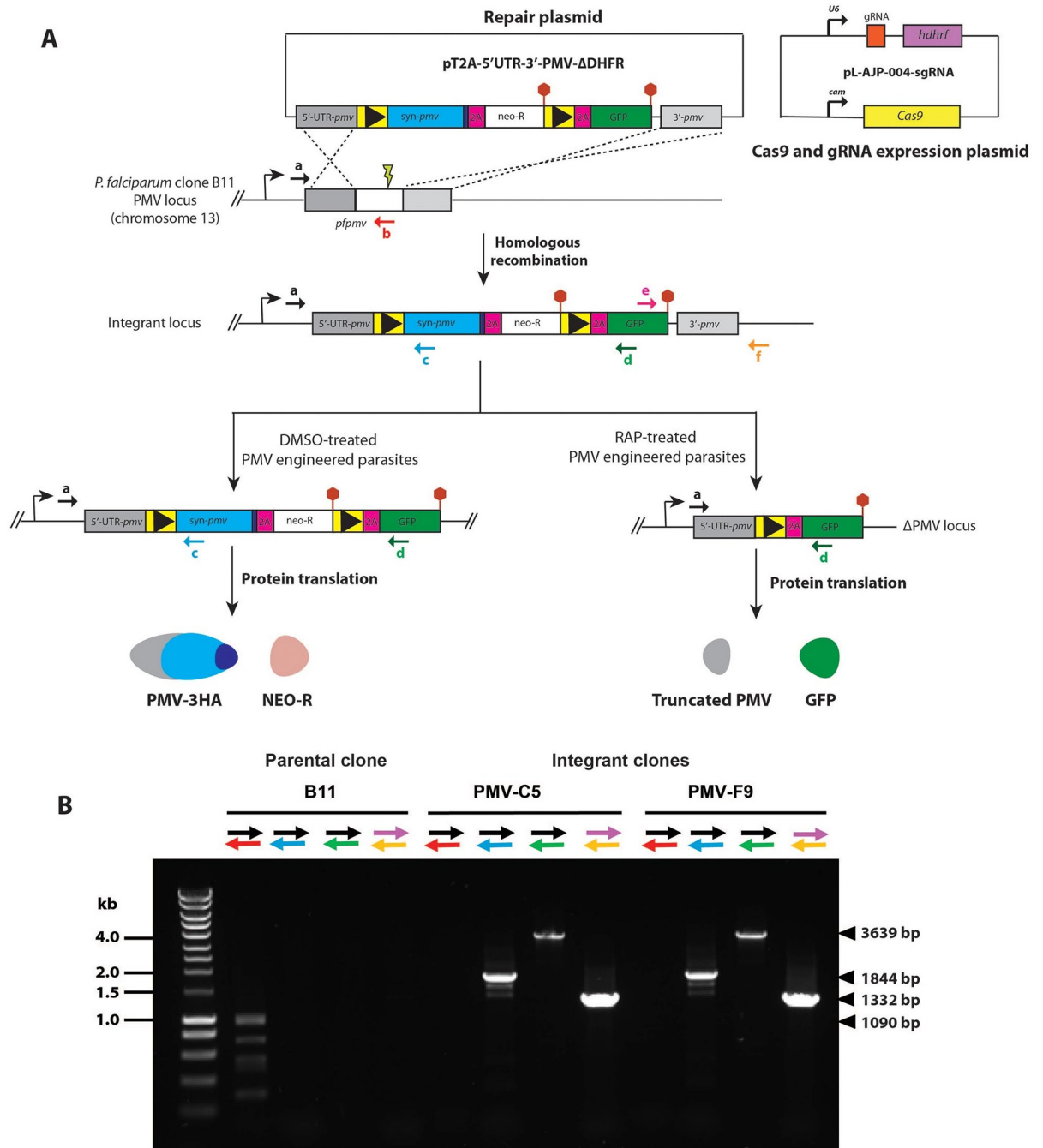


Fig 1. Generation of *P. falciparum* parasite lines expressing floxed PfPMV-HA. (A) Using a repair plasmid and Cas9-aided homologous recombination, the region of the *pfpmv* gene encoding Asp133 to Thr590 was replaced with two *loxP* (black arrowhead)-containing *P. falciparum* SERA2 introns (*loxPint*; yellow boxes) flanking a recodonised *pfpmv* gene (blue box) fused to an HA3 epitope tag (purple box), a 2A sequence (pink box), and a *neo-R* gene (white box) and stop codon (red hexagons). The second *loxPint* was also fused with 2A and *gfp* gene sequences. The *gfp* gene is translated only following site-specific recombination between the *loxP* sites by DiCre recombinase. Positions of hybridisation of primers used for confirmation of the integration event by diagnostic PCR are shown as coloured arrows. A schematic of the co-transfected plasmid for expression of Cas9 nuclease and the guide RNAs is also shown. (B) Diagnostic PCR analysis of genomic DNA of the control parental B11 and integrant *P. falciparum* clones, confirming the predicted homologous recombination event. Expected sizes of the various PCR amplicons are indicated on the right, whilst the left-hand lane contains double-stranded DNA ladder marker fragments.

<https://doi.org/10.1371/journal.pone.0207621.g001>

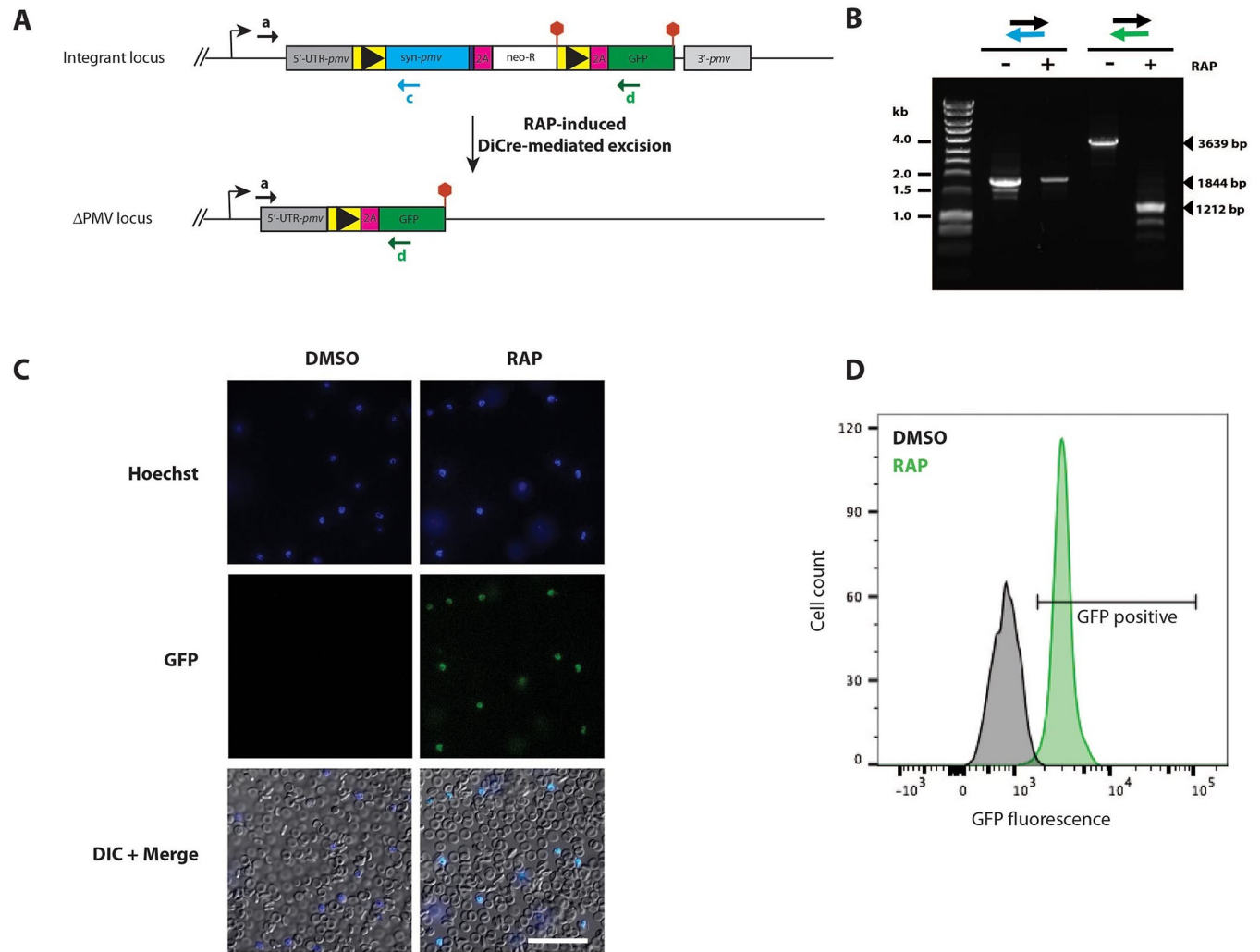


Fig 2. DiCre-mediated conditional disruption of *P. falciparum* PMV expression. (A) Predicted consequences of RAP-mediated conditional truncation of the *pfpmv* gene. Positions of hybridisation of primers used for diagnostic PCR analysis of the excision event are shown as coloured arrows. (B) PCR analysis of genomic DNA from transgenic *P. falciparum* PMV-C5 line extracted at 24 h in cycle 0 (~20 h post RAP- or DMSO-treatment), confirming the predicted DiCre-mediated excision events. Expected sizes of the PCR amplicons specific for the integrant or excised locus are indicated. A residual but much reduced signal diagnostic of the non-excised locus was also detectable in the RAP-treated parasites only with primer pair a and c, probably indicative of the high sensitivity of this PCR. Expected sizes of the various PCR amplicons are indicated on the right, whilst the left-hand lane contains double-stranded DNA ladder marker fragments. (C) Live fluorescence/DIC microscopic examination of cycle 0 PMV-C5 parasites ~42 h following treatment at ring stage with DMSO or RAP. Parasite nuclei were stained with Hoechst 33342. GFP expression was only observed in the RAP-treated population. Scale bar, 50 μ m. (D) GFP fluorescence at ~42 h in schizonts of the PMV-C5 clone treated at ring stage with DMSO or RAP, as determined by flow cytometry of fixed cultures. The percentage of GFP-positive parasites in the RAP-treated population (a reporter of excision) was 98.86%.

<https://doi.org/10.1371/journal.pone.0207621.g002>

PMV-C5 parasites was anticipated to reconstitute a single functional *loxP*-containing intron. Splicing of this intron results in a truncated form of PMV lacking the HA epitope tag, as well as allowing expression of free GFP (Figs 1A and 2A). Diagnostic PCR analysis of DNA extracted from RAP-treated and mock-treated (DMSO-treated control) PMV-C5 parasites confirmed the expected excision event (Fig 2B), although a signal indicative of some residual non-excised DNA was also detectable, as observed with some previously-described DiCre mutants (e.g. [29, 31]). To further examine this, we therefore monitored the appearance of GFP-positive parasites following treatment of synchronous ring-stage parasites with DMSO or RAP. As expected, GFP fluorescence was only detected in the RAP-treated parasites (Fig 2C).

Indeed, no schizonts lacking GFP fluorescence could be detected upon exhaustive microscopic examination of the RAP-treated cultures, indicating highly efficient excision of the floxed *pfpmv* sequence. This was supported by FACS analysis (Fig 2D), showing that nearly 99% of the RAP-treated parasites displayed GFP fluorescence. These results demonstrated close to complete conditional truncation of PMV within a single erythrocytic cycle in the PMV-C5 parasite clone.

Disruption of the *pfpmv* gene leads to a developmental arrest in the subsequent erythrocytic cycle

To initially explore the effects of PMV truncation on parasite viability, we examined growth and development of the Δ PMV mutant by microscopic examination of Giemsa-stained cultures. This revealed that although RAP-treated PMV-C5 parasites appeared morphologically normal throughout the erythrocytic growth cycle in which the parasites were treated (henceforward referred to as cycle 0), development of the mutant parasites stalled at the late ring/early trophozoite stage in the following cycle (cycle 1; Fig 3A). By the end of cycle 1, only arrested pycnotic forms were observed which did not develop further upon prolonged incubation. These results suggested that ablation of PMV expression causes a severe growth defect and developmental arrest between ring and trophozoite stage.

Whilst these results showed that truncation of PfPMV affected parasite development in cycle 1, it did not rule out the possibility of defects in egress and invasion of fresh erythrocytes at the end of cycle 0 (the cycle of RAP-treatment). To evaluate and quantify this, we used flow cytometry to monitor increases in parasitaemia at the transition between cycle 0 schizonts and cycle 1 rings. As shown in Fig 3B, the increase in parasitaemia of PMV-C5 and PMV-F9 schizont cultures at the end of cycle 0 was unaffected by RAP-treatment, indicating no effects of PMV ablation on schizont development in cycle 0, or the egress and invasion capacity of the released merozoites. However, upon further development of the new parasite generations in cycles 1 and 2, parasitaemia levels in the RAP-treated culture did not increase further. This confirmed that disruption of PfPMV did not prevent egress and invasion at the end of cycle 0, and were consistent with the Giemsa data indicating that the enzyme is essential for the ring-to-trophozoite developmental transition of the intracellular parasite in cycle 1, the cycle immediately following gene disruption.

To further explore the PMV-null phenotype, we examined the expression of PMV-HA as well as other non-exported and exported parasite proteins. Extracts of DMSO and RAP-treated PMV-C5 schizonts were analysed by immunoblot ~42 h following treatment (i.e. near the end of cycle 0), using antibodies specific for the HA epitope tag as well as GFP, the merozoite plasma membrane surface protein MSP1, and the exported protein KAHRP. As shown in Fig 4A, only a faint HA signal was detected in the RAP-treated sample, whilst a correspondingly strong GFP signal was observed only in this sample, as expected. In contrast, no differences between DMSO- and RAP-treated parasites were detectable in expression levels of the non-exported merozoite surface protein MSP1 (thought to play an important role in egress and invasion [34]) There were no obvious significant differences in expression or migration on SDS-PAGE of KAHRP, an example of a PEXEL-containing protein that is cleaved by PMV [18, 19, 21].

We next determined the effects of PfPMV truncation on its subcellular localization within the parasite, as well as on the trafficking of other exported proteins in cycle 0. Immunofluorescence analysis (IFA) showed that, as expected, PMV-HA showed a perinuclear localisation in schizonts of control PMV-C5 parasites but the signal was lost in RAP-treated parasites (Fig 4B). Mock- and RAP-treated PMV-C5 parasites were also probed with anti-MSP1 and anti-

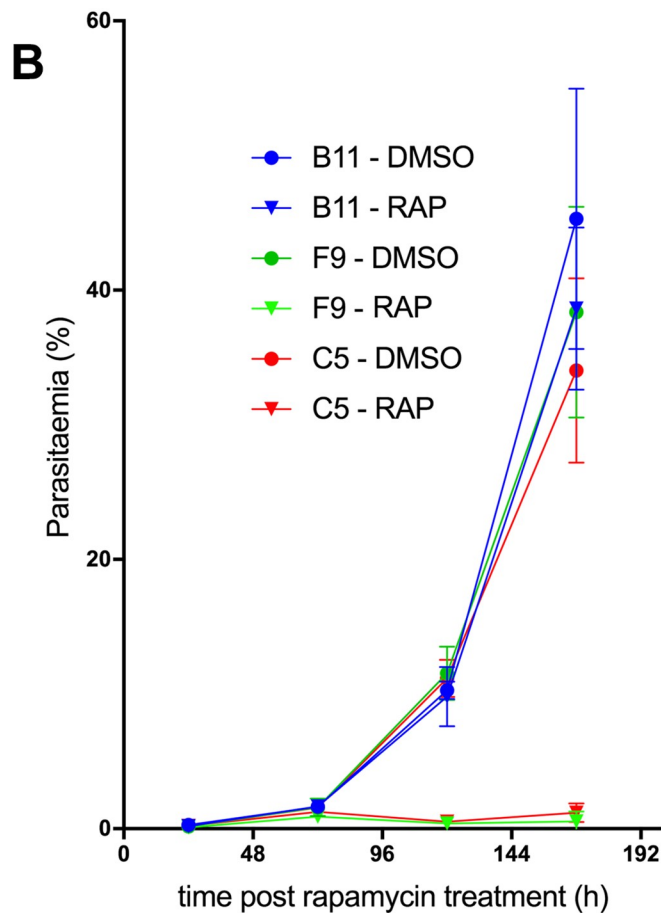
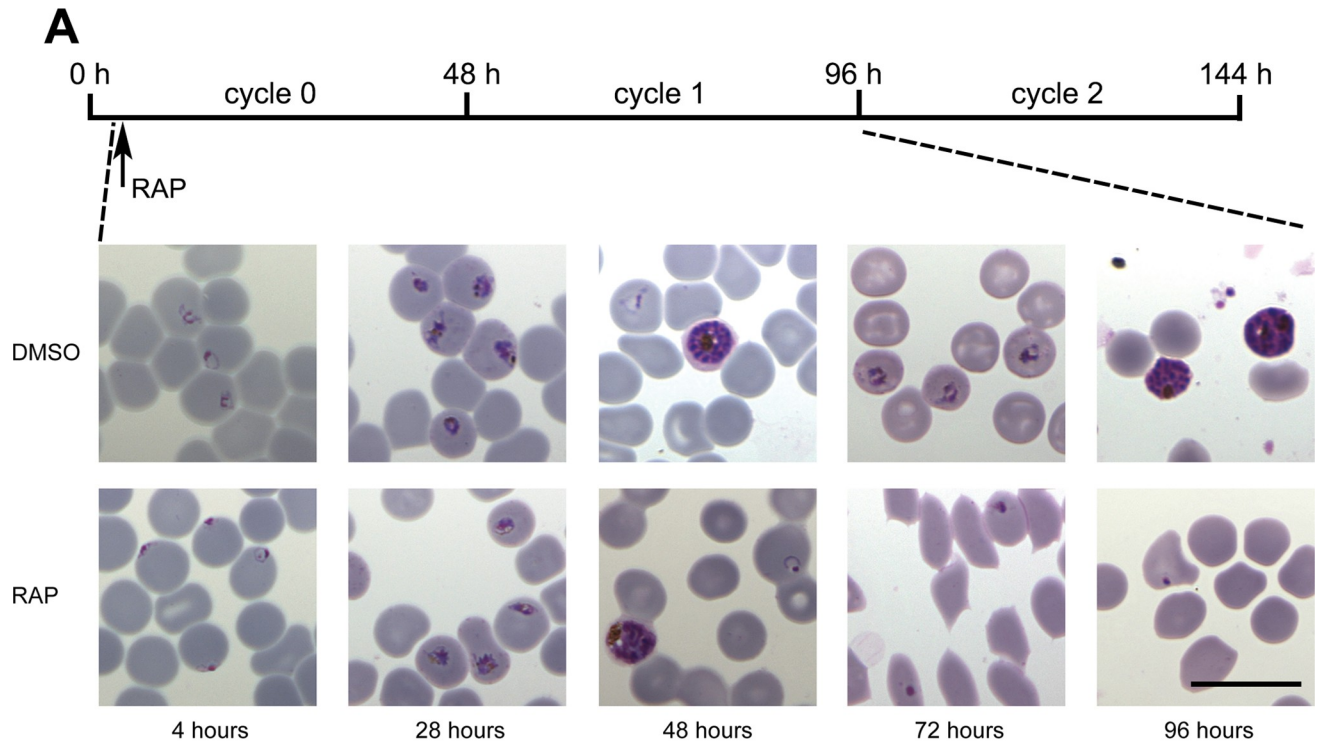


Fig 3. Functional disruption of PfPMV results in developmental arrest at the ring-to-trophozoite transition. (A) Giemsa-stained thin blood films, showing the morphology of treated PMV-C5 parasites. Scale bar, 10 μ m. The time-course of treatment and sampling of the cultures is indicated (top). (B) Growth assay showing relative replication rates following treatment of parental B11, PMV-C5 or PMV-F9 ring stage parasites with DMSO or RAP. Parasitaemia values (determined by FACS as described in Materials and Methods) are mean averages from 3 biological replicate experiments in different blood sources. The differences in growth rates between the RAP- and DMSO-treated PMV-C5 and PMV-F9 populations were extremely significant as determined by two-tailed *t*-test ($t = 11.86$, $d.f. = 10$, $P < 0.0001$). Error bars, \pm SD.

<https://doi.org/10.1371/journal.pone.0207621.g003>

KAHRP2 antibodies, as well as antibodies to another exported protein, HRP2. The localization and intensity of the MSP1 signal and the KHARP signal did not alter upon RAP-treatment, correlating well with the western blot analysis. The HRP2 signal remained detectable in both control and the RAP-treated parasites, but in contrast to the other proteins examined, the fluorescence intensity of the HRP2 signal was substantially decreased in RAP-treated parasites, suggesting a partial effect of PMV depletion on HRP2 trafficking (Fig 4B). Together, these data confirmed the loss of PMV-HA in RAP-treated parasites whilst indicating that both exported proteins (KAHRP and HRP2) and merozoite surface proteins still localised correctly in cycle 0. However, the decreased HRP2 signal intensity was consistent with a partial impact on protein export in cycle 0.

Discussion

Malarial proteolytic enzymes play regulatory and effector roles in multiple key biological processes in this important pathogen and have long been of interest as potential drug targets. In this study, we have shown for the first time that functional ablation of the *pfpmv* gene leads to a block at the ring-to-trophozoite transition and failure of the parasite to proliferate. To achieve this, we employed the robust conditional DiCre approach in combination with Cas9-induced gene modification. This system provides a rapid and efficient means of generating transgenic parasites as well as enabling complete disruption of the gene of interest [35, 36]. Our genetic strategy also incorporated a method to permit the selection of parasites in which genomic integration of the input constructs had taken place, termed selection-linked integration (SLI), previously developed by Birnbaum *et al* [32]. For this, our repair plasmid contained an SLI-resistance marker (neomycin phosphotransferase), which was linked to the modified *pfpmv* gene separated by a 2A 'skip' peptide [37, 38]. This approach allows selection for correct integration using neomycin selection. In our case, with the assistance of Cas9-mediated integration we in fact did not need to use neomycin selection in our experiments to select for correct integration. However, our plasmids could be useful for future genetic complementation studies since the *neo-R* gene is removed upon DiCre-mediated excision, effectively recycling the marker for subsequent use.

When the PMV-modified parasite clone PMV-C5 was RAP-treated at early ring stage for just 3 h, followed by removal of RAP, parasite development proceeded normally in the first erythrocytic cycle (cycle 0). Whilst expression of most of the parasite proteins examined appeared unaffected, we did observe some impact on expression of the exported parasite protein HRP2. This is reminiscent of previous observations of reductions in expression of PMV substrates following inhibition of PMV [21, 27]. We suspect that the very limited effects of *pfpmv* disruption on parasite development in cycle 0 may be due to low levels of PMV expression early in cycle 0, perhaps due to transcription early in the erythrocytic cycle prior to gene excision. That low levels of PMV are sufficient to sustain development has also been indicated by previous conditional protein knockdown experiments [27]. Egress and invasion at the end of cycle 0 was not affected in the RAP-treated PMV-C5 parasites; however, parasite development in the next cycle irreversibly stalled early following invasion. This phenotype is very similar to that observed upon treatment with the PMV inhibitor WEHI-916 [27], where the drug-

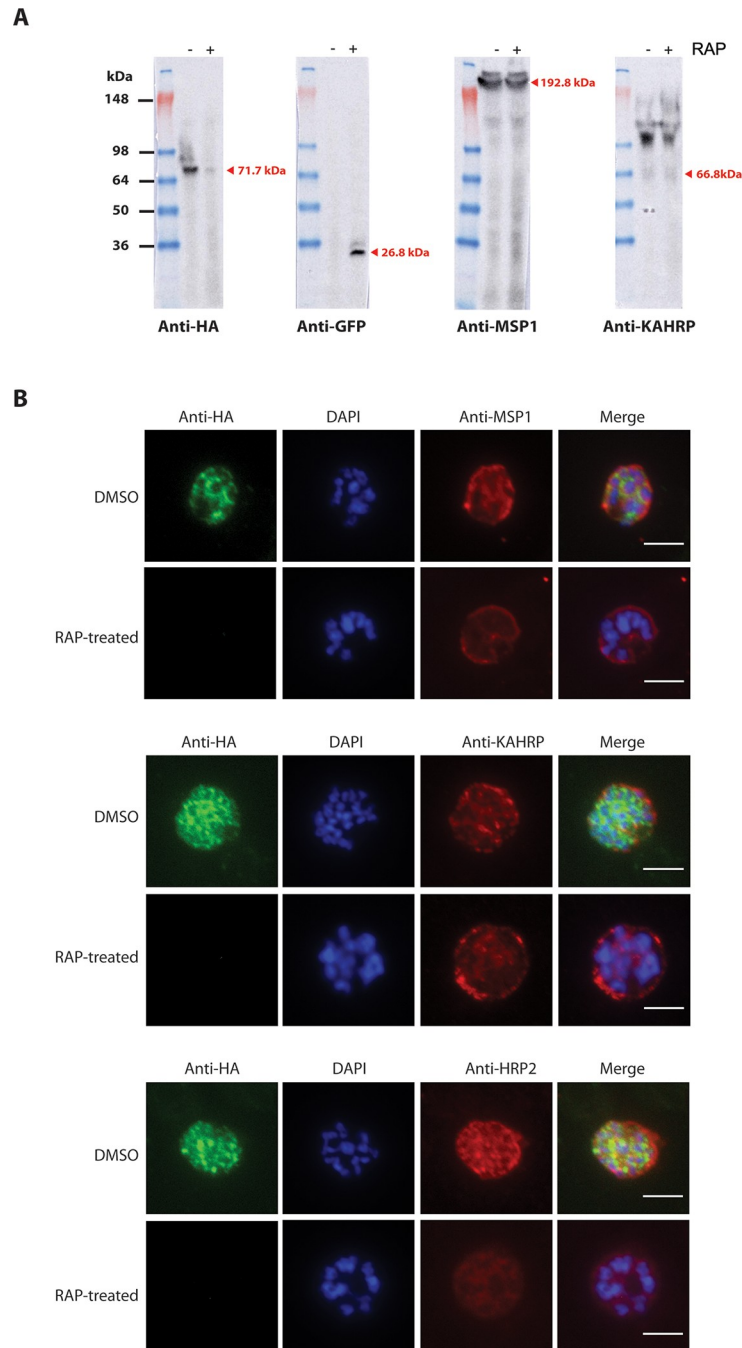


Fig 4. PMV disruption reduces expression of the exported protein HRP2. (A) Western blot analysis of equal loadings of extracts of clone PMV-C5 following DMSO (-RAP) or RAP-treatment (+RAP). Schizont extracts (~42 h post-treatment) were probed with antibodies to detect HA-tagged PfPMV (anti-HA), GFP, MSP1 (also acting as a loading control), or KAHRP. The results shown are typical of 2 separate experiments. (B) IFA of schizonts of control (DMSO-treated) and RAP-treated integrant clone PMV-C5 ~42 h following treatment (cycle 0). The PMV-HA signal was lost following RAP treatment. Localization of MSP1, KAHRP and HRP2 was unaffected; however, the HRP2 signal was significantly decreased in intensity. Parasite nuclei were visualised by staining with DAPI. Scale bars, 5 μ m. Results shown are typical of two separate experiments.

<https://doi.org/10.1371/journal.pone.0207621.g004>

treated parasites showed a growth defect at the ring-to-trophozoite transition from approximately 20 h post-invasion. A similar parasite developmental arrest at ring stage was also observed following conditional ablation of the PTEX component HSP101 [6, 7].

In summary, using a DiCre-mediated conditional gene editing approach to selectively disrupt the *pfpmv* gene, we have shown that the gene is essential for the ring-to-trophozoite transition of intracellular growth. This engineered platform will be useful for further study of PEXEL-protein export as well as for dissection of PMV domain interactions, providing further impetus for focusing on PMV as a new potential antimalarial drug target.

Materials and methods

P. falciparum culture, transfection and limiting dilution cloning

Parasites (wild type clone 3D7 and the DiCre-expressing clone B11 [33]) were routinely cultured at 37°C in human erythrocytes at 1–4% haematocrit in RPMI 1640 (Life Technologies) supplemented with 2.3 gL⁻¹ sodium bicarbonate, 4 gL⁻¹ dextrose, 5.957 gL⁻¹ HEPES, 0.05 gL⁻¹ hypoxanthine, 0.5% (w/v) Albumax II, 0.025 gL⁻¹ gentamycin sulphate, and 0.292 gL⁻¹ L-glutamine (complete medium) in an atmosphere of 90% nitrogen, 5% carbon dioxide and 5% oxygen [39, 40]. Anonymised human blood was obtained from the UK National Blood Transfusion Service. Routine microscopic examination of parasite growth was performed by fixing air-dried thin blood films with 100% methanol before staining with 10% Giemsa stain (VWR international) in 6.7 mM phosphate buffer, pH 7.1. For synchronization, mature schizont stage parasites were isolated on cushions of 70% (v/v) isotonic Percoll (GE Healthcare) as previously described [41, 42]. Enrichment for ring stages following invasion was performed using 5% (w/v) D-sorbitol [42, 43].

Cloning of repair plasmid pT2A-5'UTR-3'-PMV-ΔDHFR

pT2A-5'UTR-3'-PMV-ΔDHFR plasmid is based on vector pT2A-DDI-1cKO (a kind gift of Dr. Edgar Deu, the Francis Crick Institute). The plasmid comprised the native 5'UTR of *pfpmv* as well as nucleotides 1–397 of the native *pfpmv* sequence (Met1 to Lys132) as 5' targeting sequence for homologous recombination. This was followed by a synthetic DNA segment comprising heterologous *loxP*-containing *sera2* and *sub2* introns (*loxPint*) [31] flanking a segment of *pfpmv* sequence encoding residues Asp133 to Thr590 fused to an HA3 epitope tag sequence, a 2A 'skip' peptide (2A) [44], and the neomycin resistance gene (*neo*). The synthetic *pfpmv* sequence encoded the wild-type protein sequence but was 'recodonised' (i.e. with codon usage different to that of the native genomic parasite gene) in order to reduce its similarity at the nucleotide level with the native gene and thus prevent undesirable homologous recombination within this segment. The entire synthetic segment was produced by GeneArt. The second *loxPint* site was immediately followed by another 2A sequence, a *gfp* gene and nucleotides 1333 to 1773 of native *pfpmv* sequence which encode Lys445 to Thr590, as a 3'-targeting sequence for homologous recombination. Overlapping PCR was used to generate the *loxPint*-2A-*gfp* fragment from the template pT2A-DDI-1-cKO-complement (obtained from Dr. Edgar Deu, the Francis Crick Institute). The resulting PCR product was digested with *XhoI* and ligated into pT2A-DDI-1cKO pre-digested with the same restriction enzymes, yielding plasmid pT2A-DDI-1-cKO-modified GFP (S1 Fig). The 5'-targeting sequence (903 bp) was PCR amplified from 3D7 genomic DNA using Phusion HF DNA polymerase (NEB) with forward primer P3.1-*BglIII*_5'UTR_F-mod and reverse primer P2-Int_PMV_R. The recodonised fragment (1,602 bp) containing *loxPint*, recodonised *pfpmv*, HA3, and 2A was amplified from the plasmid 17ACRILIP_2177297_endoPMV (GeneArt) with primers P4-PMV_int_F and P5-T2A_HA_R. PCR products of 5'-target region and the recodonised

fragment were ligated with pT2A-DDI-1-cKO-modified GFP pre-digested with *Bgl*II and *Sal*I using In-fusion HD cloning kit (Clontech, Mountain View, CA), producing the plasmid pT2A-5'UTR-PMV-cKO. The 3'-target region (441 bp) was amplified from 3D7 genomic DNA using Phusion HF DNA polymerase (NEB) with forward primer P16-EcoRV-PMV-F and reverse primer P17-EcoRV-PMV-R. This fragment was then ligated into pT2A-5'UTR-PMV-cKO pre-digested with *Eco*RV, yielding the plasmid pT2A-5'UTR-3'PMV-cKO. The *hdhfr* gene was removed from pT2A-5'UTR-3'PMV-cKO by digesting the plasmid with *Bam*HI and *Eco*RI. The plasmid backbone was blunt-end using T4 DNA polymerase (NEB) then religated using T4 DNA ligase (NEB), giving rise to the repair plasmid pT2A-5'UTR-3'-PMV- Δ DHFR.

Insertion of guide RNA sequences into CRISPR/Cas9 plasmids

Potential guide RNA sequences specifically targeting *pfpmv* were identified using Benchling (<https://benchling.com/crispr>). Two sets of guide RNA sequences were selected. Two pairs of complementary oligonucleotides (P18-sgPMV-1F and P19-sgPMV-1R; P20-sgPMV-2F, and P21-sgPMV-2R) corresponding to the 19 nucleotides adjacent to the identified PAM sequences were phosphorylated using T4 polynucleotide kinase, annealed and ligated into pL-AJP_004 [45] predigested with *Bbs*I, resulting in the two guide vectors pSgRNA1 and pSgRNA2.

Generation of *pmv-loxPint* parasites and conditional PMV truncation

The repair plasmid pT2A-5'UTR-3'-PMV- Δ DHFR was linearized with *Sca*I prior to electroporation. Percoll-enriched mature schizonts of *P. falciparum* clone B11 were electroporated with 20 μ g of pSgRNA1 or pSgRNA2 and 60 μ g of linearized pT2A-5'UTR-3'-PMV- Δ DHFR using an Amaxa P3 primary cell 4D Nucleofector X Kit L (Lonza) as described [29]. Twenty-four hours post-transfection, the electroporated parasites were treated with 2.5 nM WR99210 for 96 h to select for transfectants harboring pSgRNA plasmids before returning the cultures to medium without drug. Integrant parasites generally reached parasitaemia levels suitable for cryopreservation within 2–5 weeks. Detection of the *pfpmv-loxPint* modified locus was carried out by diagnostic PCR using primer pairs P6-5'UTR_Screen_F and P23-rcPMV-5' integr-R, P6-5'UTR_Screen_F and 198_GFP_start_seq_R, and P24-GFP-3' integr-F and P25-3'UTR-PMV-R. The wild-type *pfpmv* locus was detected by diagnostic PCR using primers P6-5'UTR_Screen_F and P22-PMV-endo-R. Transgenic parasite clones were obtained by limiting dilution cloning by plating a calculated 0.3 parasite per well in flat-bottomed 96-well microplate wells as described [46]. Wells containing single plaques were subsequently expanded into round-bottomed wells. Transgenic parasite clones (PMV-C5 and PMV-F9) were finally checked by diagnostic PCR for integration and modification of the endogenous *pfpmv* gene. Once established, all transgenic clones were maintained in medium without any drug.

Recombination between the *loxPint* sites was induced in tightly synchronised ring-stages of parasite clone PMV-C5 by incubation for 3 h in the presence of 100 nM RAP in 1% (v/v) DMSO; mock treatment was with 1% (v/v) DMSO only. DiCre-mediated excision of the floxed *pfpmv* was detected by PCR analysis of parasite genomic DNA using primers P6-5'UTR_Screen_F and P23-rcPMV-5' integr-R, and P6-5'UTR_Screen_F and Deu198_GFP_start_seq_R. Truncation of *PfPMV* was evaluated by immunoblot analysis of SDS extracts of mature Percoll-enriched schizonts, probing with the anti-HA antibody 3F10 (Roche), followed by horseradish peroxidase-conjugated secondary antibodies.

Nucleic acid extraction and polymerase chain reaction

For DNA extraction, total cell pellets were first treated with 0.15% saponin in PBS for 10 min, then washed with PBS before DNA was extracted using a DNeasy Blood & Tissue Kit

(QIAGEN). For diagnostic PCR amplification, GoTaq (Promega) DNA master mix was used. Amplification of fragments used in construct design was carried out using Phusion high fidelity DNA polymerase (NEB).

Indirect immunofluorescence analysis (IFA) and Western blots

For IFA, thin blood films were prepared from synchronous *P. falciparum* cultures enriched in mature schizonts. The air-dried thin films were fixed in 4% (w/v) paraformaldehyde for 30 min, permeabilised with 0.1% (v/v) Triton X-100 for 10 min, and blocked overnight in 3% (w/v) bovine serum albumin (BSA) in PBS. Slides were probed with rat anti-HA 3F10 (1:100) to detect HA-tagged proteins, human anti-MSP1 monoclonal antibody (mAb) X509 (1:500) to detect MSP1, mAb 89 (1:100) to detect KAHRP, and mAb 2G12 (1:100) to detect HRP2. Primary antibodies were detected using Alexa Fluor 594-conjugated anti-human or anti-mouse secondary antibodies (Life Technologies), and Alexa Fluor 488-conjugated streptavidin (Life Technologies), diluted 1:2000. Slides were stained with 4,6-diamidino-2-phenylindole (DAPI), mounted in Citifluor (Citifluor Ltd., UK). Images were visualised using a Nikon Eclipse Ni microscope with LED-illumination with a 63x Plan Apo λ NA 1.4 objective. Images were taken using an Orca Flash 4 digital camera controlled by Nikon NIS Element AR 4.30.02 software. All images were subsequently analysed using FIJI software.

For Western blots, Percoll-enriched schizonts were pelleted, then resuspended into 10 volumes of PBS. Samples were solubilised into SDS sample buffer, boiled, sonicated and centrifuged. The extracts were subjected to SDS-PAGE under reducing conditions followed by transfer to nitrocellulose membrane. Membranes were probed with rat anti-HA mAb 3F10 (1:1000), human anti-MSP1 mAbs X509 (1:1000), anti-GFP (1:1000), mAb 89 (1:1000) or mAb 2G12 (1:1000), followed by horseradish peroxidase-conjugated secondary antibodies. Antigen-antibody interactions were visualised by enhanced chemiluminescence (SuperSignal West Pico chemiluminescent substrate, Pierce).

Parasite growth assay

Parasitaemia measurement by FACS was as described previously [47]. Briefly, parasites recovered at various time-points were fixed in 8% paraformaldehyde 0.04% glutaraldehyde, pH 7.4 and stained with 2 μ M Hoechst 33342 (Invitrogen, Waltham, MA). Parasitaemia was calculated using the FACS BD Fortessa flow cytometer (BD Biosciences). Cultures to be analysed were initially screened using forward and side scatter parameters and gated for erythrocytes. From this gated population, the proportion of Hoechst-stained cells in 100,000 cells was determined using ultraviolet light with a violet filter (450/50 nm). Samples were analysed using FlowJo software.

Statistical analysis

Prism 7 (GraphPad) was used for statistical analysis of growth assay data by unpaired *t*-test of biological triplicate experiments. A *P* value of <0.05 was considered statistically significant.

Supporting information

S1 Table. Oligonucleotide primer sequences used in this study.

(PDF)

S1 Fig. Construction of pT2A-DDI-1-cKO modified GFP. The *loxPint* and *gfp* fragments were amplified from pT2A-DDI-1cKO-complement. Overlapping PCR was performed to join the two fragments. The *Afl*III and *Nhe*I restriction sites were introduced to facilitate further

cloning. pT2A-DDI-1cKO was digested with *Xho*I. The digested fragment was ligated with *lox-Pint*-modified GFP fragment at the *Xho*I site.
(PDF)

Acknowledgments

The authors are grateful to Sophie Ridewood and Edgar Deu (Francis Crick Institute) for the gifts of pT2A-DDI-1 and pT2A-DDI-1-cKO-complement plasmids and for expert help with flow cytometry analysis.

Author Contributions

Conceptualization: Nonlawat Boonyalai, Christine R. Collins, Michael J. Blackman.

Formal analysis: Nonlawat Boonyalai, Christine R. Collins, Michael J. Blackman.

Funding acquisition: Michael J. Blackman.

Investigation: Nonlawat Boonyalai, Christine R. Collins, Fiona Hackett, Chrislaine Withers-Martinez.

Writing – original draft: Nonlawat Boonyalai, Christine R. Collins, Michael J. Blackman.

Writing – review & editing: Nonlawat Boonyalai, Michael J. Blackman.

References

1. WHO. World Malaria Report. 2017.
2. Haase S, de Koning-Ward TF. New insights into protein export in malaria parasites. *Cellular Microbiology*. 2010; 12(5):580–7. <https://doi.org/10.1111/j.1462-5822.2010.01455.x> PMID: 20180801.
3. Boddey JA, Cowman AF. Plasmodium nesting: remaking the erythrocyte from the inside out. *Annual Review of Microbiology*. 2013; 67:243–69. <https://doi.org/10.1146/annurev-micro-092412-155730> PMID: 23808341.
4. de Koning-Ward TF, Gilson PR, Boddey JA, Rug M, Smith BJ, Papenfuss AT, et al. A newly discovered protein export machine in malaria parasites. *Nature*. 2009; 459(7249):945–9. Epub 2009/06/19. <https://doi.org/10.1038/nature08104> PMID: 19536257; PubMed Central PMCID: PMC2725363.
5. Bullen HE, Charnaud SC, Kalanon M, Riglar DT, Dekiwadia C, Kangwanransan N, et al. Biosynthesis, localization, and macromolecular arrangement of the Plasmodium falciparum translocon of exported proteins (PTEX). *The Journal of Biological Chemistry*. 2012; 287(11):7871–84. <https://doi.org/10.1074/jbc.M111.328591> PMID: 22253438; PubMed Central PMCID: PMC3318755.
6. Beck JR, Muralidharan V, Oksman A, Goldberg DE. PTEX component HSP101 mediates export of diverse malaria effectors into host erythrocytes. *Nature*. 2014; 511(7511):592–5. Epub 2014/07/22. <https://doi.org/10.1038/nature13574> PMID: 25043010; PubMed Central PMCID: PMC4130291.
7. Elsworth B, Matthews K, Nie CQ, Kalanon M, Charnaud SC, Sanders PR, et al. PTEX is an essential nexus for protein export in malaria parasites. *Nature*. 2014; 511(7511):587–91. <https://doi.org/10.1038/nature13555> PMID: 25043043.
8. Garten M, Nasamu AS, Niles JC, Zimmerberg J, Goldberg DE, Beck JR. EXP2 is a nutrient-permeable channel in the vacuolar membrane of Plasmodium and is essential for protein export via PTEX. *Nat Microbiol*. 2018. <https://doi.org/10.1038/s41564-018-0222-7> [Epub ahead of print] PMID: 30150733
9. Ho CM, Beck JR, Lai M, Cui Y, Goldberg DE, Egea PF, et al. Malaria parasite translocon structure and mechanism of effector export. *Nature*. 2018; 561(7721):70–75. <https://doi.org/10.1038/s41586-018-0469-4> Epub 2018 Aug 27. PMID: 30150771
10. Maier AG, Rug M, O'Neill MT, Brown M, Chakravorty S, Szeszak T, et al. Exported proteins required for virulence and rigidity of Plasmodium falciparum-infected human erythrocytes. *Cell*. 2008; 134(1):48–61. <https://doi.org/10.1016/j.cell.2008.04.051> PMID: 18614010; PubMed Central PMCID: PMC2568870.
11. Elsworth B, Crabb BS, Gilson PR. Protein export in malaria parasites: an update. *Cellular Microbiology*. 2014; 16(3):355–63. <https://doi.org/10.1111/cmi.12261> PMID: 24418476.

12. Spillman NJ, Beck JR, Goldberg DE. Protein export into malaria parasite-infected erythrocytes: mechanisms and functional consequences. *Annual Review of Biochemistry*. 2015; 84:813–41. <https://doi.org/10.1146/annurev-biochem-060614-034157> PMID: 25621510.
13. Hiller NL, Bhattacharjee S, van Ooij C, Liolios K, Harrison T, Lopez-Estrano C, et al. A host-targeting signal in virulence proteins reveals a secretome in malarial infection. *Science*. 2004; 306(5703):1934–7. <https://doi.org/10.1126/science.1102737> PMID: 15591203.
14. Marti M, Good RT, Rug M, Knuepfer E, Cowman AF. Targeting malaria virulence and remodeling proteins to the host erythrocyte. *Science*. 2004; 306(5703):1930–3. <https://doi.org/10.1126/science.1102452> PMID: 15591202.
15. Spielmann T, Gilberger TW. Protein export in malaria parasites: do multiple export motifs add up to multiple export pathways? *Trends in Parasitology*. 2010; 26(1):6–10. <https://doi.org/10.1016/j.pt.2009.10.001> PMID: 19879191.
16. Heiber A, Kruse F, Pick C, Gruring C, Flemming S, Oberli A, et al. Identification of new PNEPs indicates a substantial non-PEXEL exportome and underpins common features in *Plasmodium falciparum* protein export. *PLoS Pathogens*. 2013; 9(8):e1003546. Epub 2013/08/21. <https://doi.org/10.1371/journal.ppat.1003546> PMID: 23950716; PubMed Central PMCID: PMC3738491.
17. Klemba M, Goldberg DE. Characterization of plasmepsin V, a membrane-bound aspartic protease homolog in the endoplasmic reticulum of *Plasmodium falciparum*. *Mol Biochem Parasitol*. 2005; 143(2):183–91. Epub 2005/07/19. <https://doi.org/10.1016/j.molbiopara.2005.05.015> PMID: 16024107.
18. Boddey JA, Hodder AN, Gunther S, Gilson PR, Patsiouras H, Kapp EA, et al. An aspartyl protease directs malaria effector proteins to the host cell. *Nature*. 2010; 463(7281):627–31. Epub 2010/02/05. <https://doi.org/10.1038/nature08728> PMID: 20130643; PubMed Central PMCID: PMC2818761.
19. Boddey JA, Carvalho TG, Hodder AN, Sargeant TJ, Sleebs BE, Marapana D, et al. Role of plasmepsin V in export of diverse protein families from the *Plasmodium falciparum* exportome. *Traffic*. 2013; 14(5):532–50. Epub 2013/02/08. <https://doi.org/10.1111/tra.12053> PMID: 23387285.
20. Tarr SJ, Cryar A, Thalassinou K, Haldar K, Osborne AR. The C-terminal portion of the cleaved HT motif is necessary and sufficient to mediate export of proteins from the malaria parasite into its host cell. *Molecular Microbiology*. 2013; 87(4):835–50. Epub 2013/01/03. <https://doi.org/10.1111/mmi.12133> PMID: 23279267; PubMed Central PMCID: PMC3567231.
21. Russo I, Babbitt S, Muralidharan V, Butler T, Oksman A, Goldberg DE. Plasmepsin V licenses *Plasmodium* proteins for export into the host erythrocyte. *Nature*. 2010; 463(7281):632–6. Epub 2010/02/05. <https://doi.org/10.1038/nature08726> PMID: 20130644; PubMed Central PMCID: PMC2826791.
22. Chang HH, Falick AM, Carlton PM, Sedat JW, DeRisi JL, Marletta MA. N-terminal processing of proteins exported by malaria parasites. *Mol Biochem Parasitol*. 2008; 160(2):107–15. Epub 2008/06/07. <https://doi.org/10.1016/j.molbiopara.2008.04.011> PMID: 18534695; PubMed Central PMCID: PMC2922945.
23. Boddey JA, Moritz RL, Simpson RJ, Cowman AF. Role of the *Plasmodium* export element in trafficking parasite proteins to the infected erythrocyte. *Traffic*. 2009; 10(3):285–99. Epub 2008/12/06. <https://doi.org/10.1111/j.1600-0854.2008.00864.x> PMID: 19055692; PubMed Central PMCID: PMC2682620.
24. Hodder AN, Sleebs BE, Czabotar PE, Gazdik M, Xu Y, O'Neill MT, et al. Structural basis for plasmepsin V inhibition that blocks export of malaria proteins to human erythrocytes. *Nat Struct Mol Biol*. 2015; 22(8):590–6. Epub 2015/07/28. <https://doi.org/10.1038/nsmb.3061> PMID: 26214367.
25. Sleebs BE, Gazdik M, O'Neill MT, Rajasekaran P, Lopaticki S, Lackovic K, et al. Transition state mimetics of the *Plasmodium* export element are potent inhibitors of Plasmepsin V from *P. falciparum* and *P. vivax*. *J Med Chem*. 2014; 57(18):7644–62. <https://doi.org/10.1021/jm500797g> PMID: 25167370.
26. Gambini L, Rizzi L, Pedretti A, Tagliatalata-Scafati O, Carucci M, Pancotti A, et al. Picomolar Inhibition of Plasmepsin V, an Essential Malaria Protease, Achieved Exploiting the Prime Region. *PLoS One*. 2015; 10(11):e0142509. <https://doi.org/10.1371/journal.pone.0142509> PMID: 26566224; PubMed Central PMCID: PMC4643876.
27. Sleebs BE, Lopaticki S, Marapana DS, O'Neill MT, Rajasekaran P, Gazdik M, et al. Inhibition of Plasmepsin V activity demonstrates its essential role in protein export, PfEMP1 display, and survival of malaria parasites. *PLoS Biology*. 2014; 12(7):e1001897. Epub 2014/07/02. <https://doi.org/10.1371/journal.pbio.1001897> PMID: 24983235; PubMed Central PMCID: PMC4077696.
28. Goldberg DE. Plasmepsin V shows its carnivorous side. *Nat Struct Mol Biol*. 2015; 22(9):647–8. <https://doi.org/10.1038/nsmb.3077> PMID: 26333709.
29. Collins CR, Das S, Wong EH, Andenmatten N, Stallmach R, Hackett F, et al. Robust inducible Cre recombinase activity in the human malaria parasite *Plasmodium falciparum* enables efficient gene deletion within a single asexual erythrocytic growth cycle. *Molecular Microbiology*. 2013; 88(4):687–701. <https://doi.org/10.1111/mmi.12206> PMID: 23489321; PubMed Central PMCID: PMC3708112.

30. Ghorbal M, Gorman M, Macpherson CR, Martins RM, Scherf A, Lopez-Rubio JJ. Genome editing in the human malaria parasite *Plasmodium falciparum* using the CRISPR-Cas9 system. *Nature Biotechnology*. 2014; 32(8):819–21. <https://doi.org/10.1038/nbt.2925> PMID: 24880488.
31. Jones ML, Das S, Belda H, Collins CR, Blackman MJ, Treeck M. A versatile strategy for rapid conditional genome engineering using loxP sites in a small synthetic intron in *Plasmodium falciparum*. *Sci Rep*. 2016; 6:21800. <https://doi.org/10.1038/srep21800> PMID: 26892670; PubMed Central PMCID: PMC4759600.
32. Birnbaum J, Flemming S, Reichard N, Soares AB, Mesen-Ramirez P, Jonscher E, et al. A genetic system to study *Plasmodium falciparum* protein function. *Nature Methods*. 2017; 14(4):450–6. <https://doi.org/10.1038/nmeth.4223> PMID: 28288121.
33. Perrin AJ, Collins CR, Russell MRG, Collinson LM, Baker DA, Blackman MJ. The Actinomyosin Motor Drives Malaria Parasite Red Blood Cell Invasion but Not Egress. *mBio*. 2018; 9(4). Epub 2018/07/05. <https://doi.org/10.1128/mBio.00905-18> PMID: 29970464; PubMed Central PMCID: PMC6030552.
34. Das S, Hertrich N, Perrin AJ, Withers-Martinez C, Collins CR, Jones ML, et al. Processing of *Plasmodium falciparum* Merozoite Surface Protein MSP1 Activates a Spectrin-Binding Function Enabling Parasite Egress from RBCs. *Cell Host & Microbe*. 2015; 18(4):433–44. <https://doi.org/10.1016/j.chom.2015.09.007> PMID: 26468747; PubMed Central PMCID: PMC4608996.
35. Collins CR, Hackett F, Atid J, Tan MSY, Blackman MJ. The *Plasmodium falciparum* pseudoprotease SERA5 regulates the kinetics and efficiency of malaria parasite egress from host erythrocytes. *PLoS Pathogens*. 2017; 13(7):e1006453. <https://doi.org/10.1371/journal.ppat.1006453> PMID: 28683142; PubMed Central PMCID: PMC5500368.
36. Sherling ES, Knuepfer E, Brzostowski JA, Miller LH, Blackman MJ, van Ooij C. The *Plasmodium falciparum* rhoptry protein RhopH3 plays essential roles in host cell invasion and nutrient uptake. *eLife*. 2017; 6. <https://doi.org/10.7554/eLife.23239> PMID: 28252384; PubMed Central PMCID: PMC5365315.
37. Szymczak AL, Workman CJ, Wang Y, Vignali KM, Dilioglou S, Vanin EF, et al. Correction of multi-gene deficiency in vivo using a single 'self-cleaving' 2A peptide-based retroviral vector. *Nature Biotechnology*. 2004; 22(5):589–94. <https://doi.org/10.1038/nbt957> PMID: 15064769.
38. Straimer J, Lee MC, Lee AH, Zeitler B, Williams AE, Pearl JR, et al. Site-specific genome editing in *Plasmodium falciparum* using engineered zinc-finger nucleases. *Nature Methods*. 2012; 9(10):993–8. <https://doi.org/10.1038/nmeth.2143> PMID: 22922501; PubMed Central PMCID: PMC3697006.
39. Trager W, Jensen JB. Human malaria parasites in continuous culture. *Science*. 1976; 193(4254):673–5. PMID: 781840.
40. Blackman MJ. Purification of *Plasmodium falciparum* merozoites for analysis of the processing of merozoite surface protein-1. *Methods in Cell Biology*. 1994; 45:213–20. PMID: 7707987.
41. Saul A, Myler P, Elliott T, Kidson C. Purification of mature schizonts of *Plasmodium falciparum* on colloidal silica gradients. *Bulletin of the World Health Organization*. 1982; 60(5):755–9. PMID: 6758971; PubMed Central PMCID: PMC2536039.
42. Harris PK, Yeoh S, Dluzewski AR, O'Donnell RA, Withers-Martinez C, Hackett F, et al. Molecular identification of a malaria merozoite surface sheddase. *PLoS Pathogens*. 2005; 1(3):241–51. <https://doi.org/10.1371/journal.ppat.0010029> PMID: 16322767; PubMed Central PMCID: PMC1291349.
43. Lambros C, Vanderberg JP. Synchronization of *Plasmodium falciparum* erythrocytic stages in culture. *The Journal of Parasitology*. 1979; 65(3):418–20. PMID: 383936.
44. Ryan MD, King AM, Thomas GP. Cleavage of foot-and-mouth disease virus polyprotein is mediated by residues located within a 19 amino acid sequence. *The Journal of General Virology*. 1991; 72 (Pt 11):2727–32. <https://doi.org/10.1099/0022-1317-72-11-2727> PMID: 1658199.
45. Knuepfer E, Napiorkowska M, van Ooij C, Holder AA. Generating conditional gene knockouts in *Plasmodium*—a toolkit to produce stable DiCre recombinase-expressing parasite lines using CRISPR/Cas9. *Sci Rep*. 2017; 7(1):3881. <https://doi.org/10.1038/s41598-017-03984-3> PMID: 28634346; PubMed Central PMCID: PMC5478596.
46. Thomas JA, Collins CR, Das S, Hackett F, Graindorge A, Bell D, et al. Development and Application of a Simple Plaque Assay for the Human Malaria Parasite *Plasmodium falciparum*. *PLoS One*. 2016; 11(6):e0157873. <https://doi.org/10.1371/journal.pone.0157873> PMID: 27332706; PubMed Central PMCID: PMC4917082.
47. Stallmach R, Kavishwar M, Withers-Martinez C, Hackett F, Collins CR, Howell SA, et al. *Plasmodium falciparum* SERA5 plays a non-enzymatic role in the malarial asexual blood-stage lifecycle. *Molecular Microbiology*. 2015; 96(2):368–87. <https://doi.org/10.1111/mmi.12941> PMID: 25599609; PubMed Central PMCID: PMC4671257.